THE EXPLOITATION OF TITANIUM DIOXIDE NANOPARTICLES FOR IMPROVING THE PERFORMANCE AND EMISSIONS OF BIOFUEL-DIESEL BLEND-FUELLED STATIONARY DIESEL ENGINE

Abdülvahap ÇAKMAK *

Abstract: In this research, the potential effects of titanium dioxide (TiO_2) nanoparticles on improving a stationary diesel engine characteristic fuelled with a biofuel mixture-diesel blend (B25: 25% vol. biofuel mixture containing biodiesel, waste cooking oil and ethanol + 75% vol. diesel) are experimentally investigated. TiO_2 nanoparticles are dispersed in B25 fuel at 50, 100, and 150 ppm concentrations. Subsequently, they are tested in a stationary research diesel engine at a rotational speed of 1500 rpm and specific loads. Nanoparticles enhance combustion, offering increased cylinder gas pressure, net heat release rate, and reduced ignition delay period and combustion duration. The engine performance is enhanced more with increasing nanoparticle concentration. TiO_2 nanoparticles with a 150 ppm rate reduce brake-specific fuel consumption by 3.21% and increase the brake effective efficiency by 3.67%, on average, compared to B25 fuel without nanoparticles. CO emission and smoke opacity are reduced by up to 31.89% and 24.56% with TiO_2 nanoparticles. However, under the same operating conditions, NO emission increases to 30.58% compared to sole B25. Nevertheless, the NO emission of nanofuels is still less than that of diesel fuel. This study's results indicate that using TiO_2 nanoparticles as a nano fuel additive can enhance the stationary engine's operation fueled with the biofuel mixture-diesel blend.
Keywords: Biofuel, Diesel engine, Fuel additive, Nanoparticles

Biyoyakıt-dizel karışımı ile çalışan stasyoner dizel motorunun performans ve emisyonlarını iyileştirmek için titanyum dioksit nanopartiküllerinin kullanılması

Özet: Bu araştırmada titanyum dioksit (TiO_2) nanopartiküllerinin, biyoyakıt-dizel karışımı (B25: biyodizel, atık kızartma yağı ve etanol içeren %25 hacimli biyoyakıt karışımı + %75 dizel) ile çalışan stasyoner dizel motorunun performans ve emisyonlarını iyileştirme potansiyeli deneysel olarak incelenmiştir. TiO_2 nanopartikülleri B25 yakıtına 50, 100 ve 150 ppm konsantrasyonlarında eklenmiştir. Elde edilen nanoyakıtlar, stasyoner bir dizel motorda 1500 d/dk dönüş hızında ve farklı yüklerde test edilmiştir. Nanopartiküller yanmayı iyileştirerek, silindir basıncını ve net ısı yayılım oranını artırmış, tutuşma gecikmesi süresi ile yanma süresini kısaltmıştır. Nanopartikül konsantrasyonu arttıkça motor performansı daha da iyileşmiştir. 150 ppm oranındaki TiO_2 nanopartikülleri, nanopartikül içermeyen B25 yakıtına kıyasla özgül yakıt tüketimini %3,21 oranında azaltmış ve efektif verimi ortalama %3,67 oranında artırmıştır. TiO_2 nanopartikülleri kullanımı ile CO emisyonu ve duman koyuluğu %31,89 ve %24,56'ya kadar azalmıştır. Bununla birlikte, aynı çalışma koşullarında NO emisyonu, nanopartikül içermeyen B25 yakıtına kıyasla %30,58'e kadar artmıştır. Ancak nanoyakıtlar dizel yakıtına göre daha az NO emisyonu oluşturmuştur. Bu çalışmanın sonuçları, TiO_2 nanopartiküllerinin nano yakıt katkısı olarak kullanılmasının biyoyakıt-dizel karışımıyla çalışan stasyoner dizel motorun performans ve emisyonlarını iyileştirebileceğini göstermektedir.
Anahtar Kelimeler: Biyoyakıt, Dizel motor, Yakıt katkısı, Nanopartikül

1. INTRODUCTION

* Samsun University, Faculty of Engineering, Mechanical Engineering Department, Ballica Campus, Tekel Cd., 55420, Ondokuzmayıs/Samsun
Corresponding Author: Abdülvahap Çakmak (abdulvahap.cakmak@samsun.edu.tr)

Stationary diesel engines run on a constant engine rotation speed to generate electricity or power mechanical equipment, such as pumps or compressors. They are powered by various fuels, mainly fossil diesel, heavy fuel oil, and natural gas. However, challenges such as the oil crisis, unstable fuel prices, and environmental and health issues resulting from fossil fuel consumption make using renewable energy sources indispensable (Kumar, 2020). Accordingly, the research for new alternative energy sources and the use of available renewable fuels has attracted much attention since they offer many benefits of being renewable and sustainable fuels, reducing environmental concerns, being produced from domestic sources, diversifying fuel supply, reducing dependence on foreign oil, and ensuring energy security (Hadhoum et al., 2021).

Biodiesel and ethanol derived from wastes or non-edible sources have become more appealing due to their economic availability and technical feasibility (Agarwal, 2007). Therefore, applying biodiesel and alcohols with diesel fuel has been extensively examined. Some studies report that biofuel-diesel blends with 10-20% biofuel fraction offer comparable results with neat diesel fuel (Khan et al., 2022; Niculescu et al., 2019). On the other hand, some studies concluded that diesel-biodiesel-binary blends or diesel-biodiesel-alcohol ternary blends could perform better results regarding pollutants emissions such as CO, HC, and PM but poor engine performance and increased NO_X emissions. For example, in a recent study (Gülüm, 2023), 1-butanol and 1-pentanol are mixed with raw corn oil-diesel blend by 4%, 7%, and 10% by volume to obtain ternary blends and investigated on a diesel engine. For ternary blends, CO, HC, and smoke opacity decrease while NOx increases compared to diesel. Moreover, it is found that engine efficiency decreases up to 4.05% with ternary fuel blends owing to their lower calorific value than diesel fuel. Santhosh et al. (2023) conducted a research study evaluating the performance of a diesel engine fuelled with poultry fat diesel-biodiesel-ethanol blends. Three fuel blends with a fixed biodiesel fraction of 10% and a varying ethanol fraction from 5% to 15% by volume are obtained and subjected to engine tests. Diesel fuel and neat biodiesel are employed as baseline fuels. Engine performance characteristics are improved by the inclusion of ethanol by 5% into the biodiesel-diesel blend. Thanks to its low viscosity, ethanol improves thermal efficiency compared to biodiesel fuel and gives almost the same efficiency as diesel fuel. Biodiesel-ethanol-diesel blends reduce CO, HC, and NO_X emissions. Nevertheless, adding ethanol beyond 5% volume in the biodiesel-diesel blend does not perform any achievement in engine performance. Contrarily, as increasing the ethanol ratio, thermal efficiency reduces, and the fuel flow rate into the cylinder increases owing to its lower calorific value.

Long-chain alcohols have higher cetane number, high energy density, less corrosive effect on fuel system parts, and better phase stability than short-chain alcohols. Therefore, long-chain alcohols have come to the front as alternative fuels that can be blended with diesel or biodiesel (Suhaimi et al., 2018). In a new study concluded by Yibaşi et al. (2023), pentanol, hexanol, and butanol were blended one by one in three different proportions of 10%, 20%, and 30% volumetrically with diesel-hemp seed oil methyl ester and tested in a direct injection engine operated at different loads. It is found that as the increase in long-chain alcohol concentration in the fuel mixture, the ignition delay prolongs due to a decrease in the cetane number of the fuel blend. Smoke opacity, NO_X, CO, and HC decrease for all types of alcohol used, and these emissions are further reduced for a higher alcohol blending ratio. However, in this case, at the same running conditions, the engine performance is worsened due to a reduction in heating value and cetane numbers of ternary blends as well as an increase in the heat of vaporization. Consequently, it is concluded that comparable engine performance with lower pollutant emissions can be obtained for a lower alcohol blending ratio.

Table 1. Review of some studies dealing with the effects of nanoparticles on engine parameters

Ref.	NPs type	NPs concentration	Base fuel	Test engine/test conditions
(Yusuf et al., 2022)	Al_2O_3 + TiO_2	20, 40, and 60 ppm	n-butanol + waste plastic oil + diesel	6-cylinder, 4-stroke, common-rail diesel engine/1700 rpm and 75% load
	Remarks	Reduced unregulated emissions of hexadecane, tetradecane, dodecane, and octadecane are detected. Lower CO and HC but higher NO_X are recorded. The combustion process is shortened, and heat release is fastened due to the strong oxidation effect of hybrid nanoparticles.		
(Örs et al., 2018)	TiO_2	0.01% on a mass basis	Diesel + waste cooking oil biodiesel + n- butanol	4-stroke 1-cylinder, water-cooled, diesel engine/ at full throttle position and 1000-3000 rpm
	Remarks	Engine torque and power increase by about 9.74% while fuel consumption diminishes by 28.37% compared to fuel blend without nanoparticles. HC, CO, and smoke opacity decrease while CO_2 and NO_X increase due to the improvement in combustion quality with TiO_2 nanoparticles.		
(Venu et al., 2021)	Al_2O_3	10, 20, and 30 ppm	diesel (70%) + Jatropha biodiesel (20%) + ethanol (10%)	4-stroke, 1-cylinder, naturally aspirated compression ignition engine/ at 1500 rpm and 25-100% load
	Remarks	Combustion characteristics enhance. Smoke emissions, NO_X, HC, and CO and brake-specific fuel consumption decrease while brake thermal efficiency increases by adding Al_2O_3 nanoparticles to the ternary blend. The optimum nanoparticle concentration is found to be 20 ppm.		
(Uslu et al., 2023)	TiO_2	25, 50, 75, and 100 ppm	hemp seed oil biodiesel-diesel blend (B30)	single-cylinder diesel engine/ operated at a constant rotational speed of 3000 rpm and different loads of 1.5, 2.0, 2.5, and 3.0 k W
	Remarks	100 ppm TiO_2 nanoparticles lead to an increase in thermal efficiency and a decrease in specific fuel consumption by 5.16%. The optimum TiO_2 concentration is found to be 75 ppm. In addition, while CO and HC emissions are reduced, NO_X emissions rise by 27% on average.		

The review reports show that although a notable reduction in exhaust emissions can be accomplished with a higher biofuel ratio, engine performance is well below that of diesel-biofuel blends with lower biofuel proportions or diesel. It indicates a trade-off between performance and exhaust emissions for the increasing biofuel ratio in the mixture. Therefore, the existing trade-off should be improved to expand biofuel's share in the mixture. Fortunately, nanoparticles (NPs) have emerged as suitable fuel additives due to their benefits in exhaust emissions and engine performance. Including various nanoparticles in base fuel can enhance

physicochemical fuel properties, improving engine performance and emissions. The performance enhancer aspect of nanoparticles is primarily ascribed to their high thermal conductivity, high chemical activity, large surface area, high energy density, oxygen content, and mass diffusivity (Hoang, 2021). Some studies examining the impacts of nanoparticles on engine parameters and the significant findings from these studies are summarized in Table 1.

Using a combination of biofuels derived from various feedstock instead of a type of biofuel can be a viable option to extend the use of biofuels in the market. Also, such an approach makes it possible to take more advantage of waste oils and domestic feedstocks. Because feedstock availability for biofuel production varies regionally and seasonally, only one feedstock may not continuously supply the increasing biofuel demand (Çakmak, 2022). It constitutes the motivation for this presented research. Accordingly, this research prepares and tests a quaternary fuel blend of canola oil biodiesel-waste cooking oil-ethanol-diesel fuel in the engine. The biofuel mixture proportion is fixed at 25% by volume in the biofuel mixture-diesel blend. It is slightly higher than the commonly used biofuel blending ratio of 20%. Considering the projections for the gradual transition to fully renewable energy, the blending proportion of biofuels with fossil fuels will increase in the coming years. For example, the European Union targets to increase the biofuel share up to at least 27% in total energy consumption in transportation by 2030 (European Commission, 2014). Based on this issue, the biofuel blending ratio is over 20%. Besides, the preliminary experimental investigations with biofuel mixture/diesel fuel blends have indicated that the optimum biofuel ratio is 25% by volume; however, its engine performance is poor compared to diesel fuel. Therefore, this experimental study aims to improve its performance and emission characteristics by employing TiO_2 nanoparticles as a performance enhancer additive. TiO_2 nanoparticles are dispersed by mechanical mixing and ultrasonication process on the biofuel mixture-diesel blend by 50, 100, and 150 ppm mass concentration. After that, the obtained test fuels' physicochemical properties are measured by standard test methods. Subsequently, engine tests are done to investigate the impacts of TiO_2 nanoparticles on engine operating parameters.

Diesel fuel and the biofuel mixture-diesel blend without nanoparticles are employed as reference fuels to compare the findings. The results are graphically presented and analyzed in detail in the result and discussion section. The improved engine performance and lowered exhaust emissions of quaternary fuel blends with TiO_2 nano additives are accomplished, allowing the blending of biofuels with diesel fuel in greater proportions. Besides, the obtained findings could guide the use of a combination of various biofuels.

2. MATERIALS AND METHODS

Ultra-low sulfur diesel fuel (ULSD), canola oil biodiesel, waste cooking oil, ethanol, and TiO_2 nanoparticles are used to prepare test fuels. ULDS that meets the TS EN 590 standards is purchased from a fuel station (OPET) in Samsun. A domestic licensed commercial biodiesel producer supplies biodiesel, and it meets the European biodiesel standard (EN 14214). The biodiesel fuel specification can be found elsewhere (Çakmak et al., 2022). Ethanol, with a purity of 99.5%, is provided by a chemical company (TEKKİM). Waste cooking oil is obtained from the school canteen and pre-treated before use. In pre-treatment, filtering is performed first to screen out solid particles present in the oil. Then, the oil is heated to 110 °C in a glass beaker and stirred for 30 minutes to evaporate the existing water in the oil. Lastly, it is filtered again and made ready for use. TiO_2 nanoparticles with 30-40 nm particle size are purchased from NanoAmor Incorporation (USA), and the characterization of TiO_2 nanoparticles is performed by scanning electron microscope (SEM). Figure 1 shows the SEM image of TiO_2 nanoparticles at a magnification of 15,000 x. The average particle size of TiO_2 nanoparticles is 30-40 nm, significantly lower than the diameter of the fuel injector nozzle hole (=0.24 mm). Therefore, it does not cause injector clogging.

Biofuel mixture is prepared by mixing canola oil biodiesel, waste cooking oil, and ethanol by 60%, 20%, and 20% on a volumetric base. Then, the obtained biofuel mixture is blended with diesel fuel in the volumetric percentage of 25:75, yielding a biofuel mixture-diesel blend defined as B25. Diesel fuel (DF) and B25 fuel are reference fuels in the engine tests. TiO_2 nanoparticles are directly added as particulate (solid particles) to B25 fuel. No surfactant is used to avoid its impact on combustion and thus determine the net effects of the TiO_2 nanoparticles. The mass of TiO_2 nanoparticles is measured by a digital analytical balance with a precision scale of 0.1 mg. TiO_2 nanoparticles are dispersed in B25 by 50, 100, and 150 ppm mass concentration to acquire nanofuels labeled as B25+NPs50, B25+NPs100, and B25+NPs150, respectively. TiO_2 nanoparticles with a measured amount are added to the B25 fuel and thoroughly stirred with a magnetic stirrer at 500 rpm for 15 minutes. Subsequently, nanofuels are homogenized by an ultrasonic probe sonicator at 40 Hz for 15 minutes. All nanofuels are stable, and there is no phase separation or sedimentation for two hours after preparation. Figure 2 illustrates the photography of fuel samples. The same basic properties of the test fuels are measured by following the standard given elsewhere (Çakmak and Özcan, 2022), and the results are presented in Table 2.
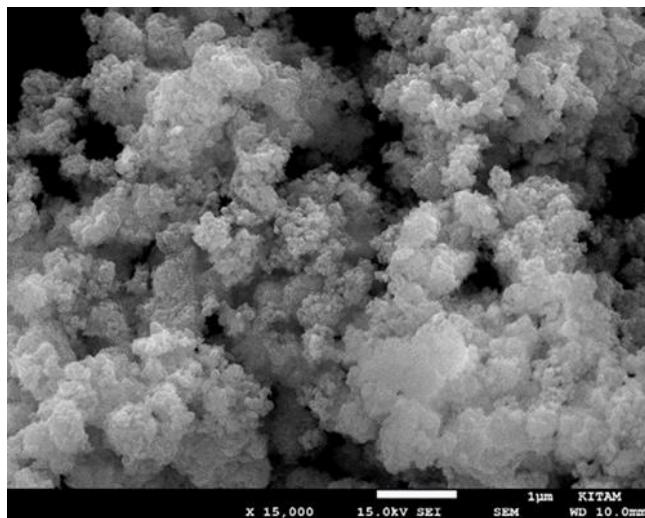

Figure 1:
SEM image of TiO₂ nanoparticles captured at a magnification of 15,000.

Figure 2:
The image of the test fuel samples.

Figure 3 represents schematically the arrangement of the test rig. A single-cylinder, four-stroke cycle, and direct-injection stationary diesel engine, the TV1 Kirloskar model engine, is utilized in this study. Its displacement volume is 0.6615 liter with a bore and stroke length of 87.5x110 mm. The engine is rated at 3.5 kW at 1500 rpm and develops 21.8 Nm of torque at the same speed. It is a naturally aspirated diesel engine with the start of fuel injection of 23 crank angle degrees (°CA) before the top dead center (bTDC) and a compression ratio of 17.5:1. An Eddy-current type dynamometer with an absorption power of 10 kW is used for measuring engine torque. The crankshaft speed is measured from a shaft-mounted rotary encoder. A piezoelectric transducer and crank angle encoder monitor the engine cylinder pressure. Fuel flow rate and air flow rate are measured by differential pressure transmitters. The exhaust gas temperature on the exhaust manifold and exhaust gas calorimeter inlet/outlet is measured with K-type thermocouples. The exhaust gas is analyzed by the BOSCH BEA 060 five-gas analyzer, and the opacity of the exhaust gas is detected by the BOSCH BEA 060 smoke opacity measurement device. The specifications of test instruments are listed in Table 3.

Table 2. Measured fuel properties.

Property (Unit)	DF	B25	B25+NPs50	B25+NPs100	B25+NPs150
Density @15 °C (kg/m³)	828.6	839.3	839.2	839.3	839.5
Kinematic vis.(mm²/s) @40°C	2.58	2.95	2.94	2.96	2.99
Water content % (m/m)	0.004	0.059	0.060	0.056	0.057
Sulfur content (mg/kg)	6.1	5.3	5.4	5.3	5.2
CFPP (°C)	-20.0	-16.0	-16.0	-16.0	-16.0
Flashpoint (°C)	63.0	24.0	24.0	24.0	24.0
Cetane index	55.5	53.4	53.7	53.6	54.1
Recovery at 250°C % (v/v)	36.3	30.7	30.6	30.5	30.4
Recovery at 350°C % (v/v)	94.2	91.6	91.4	90.7	91.0
95% (v/v) Recovery °C	352.9	355.3	355.1	357.0	356.5
First boiling temperature (°C)	163.1	77.5	77.4	77.0	77.6
Last boiling temperature (°C)	364.0	357.8	355.6	357.8	356.9

Engine brake power in kW unit is determined by multiplying the measured brake torque (Nm) by the angular velocity (s^{-1}) of the crankshaft:

$$P_B = T_B \times \omega \times 10^{-3} \qquad (1)$$

Brake-specific fuel consumption is the ratio of fuel consumption rate to brake power produced in the unit of kg/kWh:

$$bsfc = \frac{\dot{m}_f}{P_B} \qquad (2)$$

Where: $\dot{m}_f$ is the fuel consumption rate of the engine (kg/h). Brake-mean effective pressure (bmep) in the unit of kPa is obtained:

$$bmep = \frac{T_B \times 4\pi}{V_s} \times 10^{-3} \tag{3}$$

where V_s is the stroke volume (m³). Brake effective efficiency (fuel conversion efficiency) indicates the conversion rate of fuel energy to brake power and is computed as follows:

$$\eta = \frac{3600}{bsfc \times Q_f} \times 100 \tag{4}$$

here Q_f is the lower calorific value of the fuel in the unit of kJ/kg.

The combustion parameters are obtained by processing the cylinder gas pressure-crank angle data captured over 100 sequential cycles in the LabVIEW-based software package (ICEngineSoft, Version 9.0). Based on the first law of thermodynamics and equation of state, the net heat release rate (NHRr) is determined by implementing Equation (5) (Heywood, 1988):

$$\frac{dQ_n}{d\theta} = \frac{1}{k-1}\left[kP\frac{dV}{d\theta} + V\frac{dP}{d\theta}\right] \tag{5}$$

Where: P is the measured cylinder gas pressure in the unit of kPa, V is the instantaneous cylinder volume in the unit of m^3, and k is the specific heat ratio of the gases inside the cylinder.

The pressure rise rate (PRr) is given by:

$$PRr = \frac{dP}{d\theta} \tag{6}$$

Cumulative heat release (CHR) is figured out as follows:

$$CHR = \int \frac{dQ_n}{d\theta} \tag{7}$$

The ignition delay period lasts from the beginning of fuel injection to the start of combustion (CA$_{10}$). The total combustion duration is from CA$_{10}$ to CA$_{90}$. CA$_{10}$ and CA$_{90}$ are crank angles at which 10% and 90% cumulative heat release appear. The normalized values of the cumulative heat release are used to define the combustion phases.

Diesel fuel, B25, B25+NPs50, B25+NPs100, and B25+NPs150 are systematically subjected to engine tests. Engine tests are carried out at 1500 rpm, and brake mean effective pressure of 0.1, 0.2, 0.3, and 0.4 MPa. These loads correspond to 25% (low), 50% (mid), 75% (high), and 100% (full) engine loads, respectively. All measurements are recorded after the engine reaches stable running conditions. The average value of four readings for performance and emissions is considered to increase the accuracy of the results. The uncertainty of the performance parameters is calculated by Equation (8):

$$U_P = \pm\left[\sum_{i=1}^{n}\left(\frac{\partial P}{\partial x_i}u_i\right)^2\right]^{1/2} \tag{8}$$

where U_P is the calculated uncertainty, P is the dependent variable of x with the uncertainty of u. The uncertainty analysis results are given in Table 4.

Table 3. The technical specifications of test instruments

Measured Parameter	Resolution	Measuring range	Accuracy
Engine speed sensor	1 rpm	0-9999 rpm	$\pm$10 rpm
Crank angle sensor	1°	0-360°	$\pm$1°
Cylinder pressure sensor	0.7 kPa	0-34.5 MPa	$\pm$0.01 MPa
Temperature sensor	0.1°C	0-1200 °C	$\pm$0.5 °C
CO	0.001 % vol.	0-10 % vol.	$\pm$0.005 % vol.
CO_2	0.01 % vol.	0-18 % vol.	$\pm$0.5 % vol.
NO	1 ppm	0-5000 ppm	$\pm$ 5 ppm
Smoke opacity	0.1 %	0-100 %	$\pm$1%
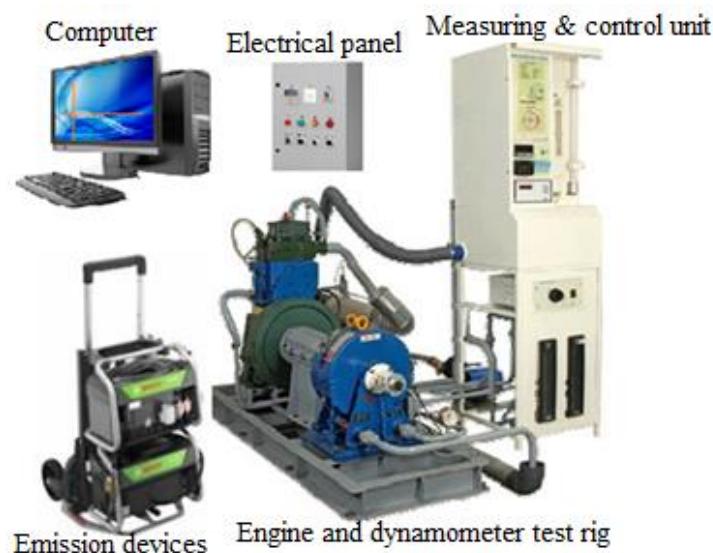
Figure 3:
Schematic view of the experimental test setup.

Table 4. Uncertainty of the performance parameters calculated at bmep of 0.4 MPa.

Parameter	Uncertainty	Fractional uncertainty
Brake power	$\pm$ 0.0161 kW	$\pm$0.4647%
Fuel consumption rate	$\pm$0.0050 kg/h	$\pm$0.6430%
Brake-specific fuel consumption	$\pm$0.0018 kg/kWh	$\pm$0.7933%
Brake effective efficiency	$\pm$0.0033 (-)	$\pm$0.9403%

3. RESULTS AND DISCUSSION

3.1 Combustion Analysis

The heat release rate is an indicator of the burning rate of the fuel. The trend of heat release rate curves is nearly similar for all fuels tested, as seen in Figure 4. However, the maximum value of the heat release rate is different. The highest value of the heat release rate of 41.92 J/degree belongs to B25+NPs50 ppm, while the lowest one by 20.92 J/degree, is observed for B25 fuel. Besides, nanoparticle-incorporated fuels produce a greater heat release rate than diesel fuel. The thermophysical properties of the fuel affect mixture formation and combustion inside the cylinder. With B25 fuel, the heat release rate is the lowest due to high viscosity, low volatility, and high density, adversely impacting fuel atomization, evaporation, and, eventually, combustion. Diesel fuel with high energy density and low viscosity performs better combustion and a higher heat release rate than B25. Nanoparticle-doped fuels could enhance fuel atomization, evaporation, and combustion thanks to their substantial surface area, high thermal conductivity, and ability to increase the rate of chemical reaction. Consequently, with the presence of nanoparticles in fuel, the combustion accelerates, thereby increasing the heat release rate. B25+NPs100 and B25NP150 present a lower heat release rate than B25+NPs50. It may be due to a shorter ignition delay for 100 and 150 ppm TiO_2 concentrations. The shorter ignition delay period can reduce the amount of fuel burned in the premixed combustion phase, resulting in a lower heat release rate.
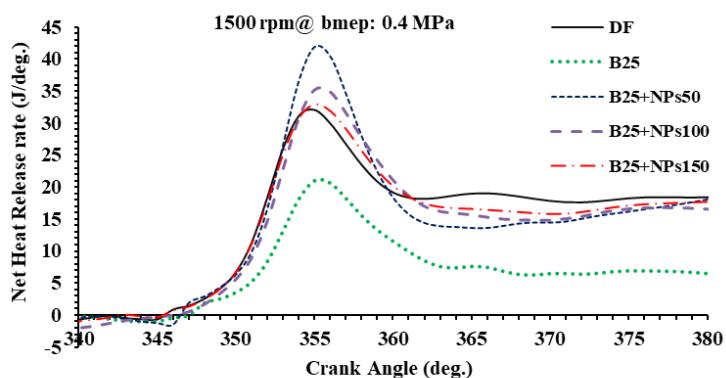

***Figure 4**:*
Net heat release curve of test fuels

Figure 5 presents the cylinder pressure curve of test fuels. The overall shape of cylinder pressure curves, as well as the peak values, do not differ to a great extent. The maximum cylinder pressure for DF, B25, B25+NPs50, B25+NPs100, and B25+NPs150 is 5.33, 5.30, 5.38, 5.53, and 5.43 MPa, respectively. Besides, the location of the peak cylinder pressure is advanced by 2 °CA for nanofuels compared to diesel fuel because TiO_2 nanoparticles positively impact combustion. It is noted that all fuels are tested at the same brake power output. Therefore, an engine running on fuel blends with lower calorific value than diesel fuel consumes more fuel during the cycle, resulting in closer cylinder pressure values to each other. On the other hand, the increasing tendency of cylinder pressure for nanoparticle-added fuels is remarkable. It may be attributed to the specific properties of nanoparticles and their favorable effect on mixture formation and combustion.
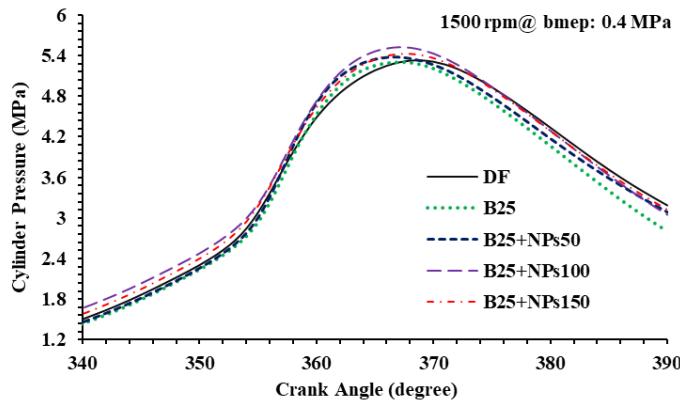
Figure 5:
Cylinder pressure curve of test fuels.

Figure 6 shows the determined pressure rise rate for test fuels at an engine load of 0.4 MPa. B25+NPs50 fuel shows a maximum pressure rise rate of 0.386 MPa/degree (=3.501 MPa/ms), while DF shows a minimum pressure rise rate of 0.309 MPa/degree (=2.781 MPa/ms). The maximum pressure rise rate values of the remaining fuels are between the values of the B25+NPs50 and DF. The reason for the maximum pressure rise rate with B25+NPs50 fuel is the increased combustion rate, which is confirmed by its heat release rate curve. However, B25 fuel with the lowest peak heat release rate presents a higher pressure rise rate than diesel and nanofuels with 100 and 150 ppm TiO_2 concentrations. It can be ascribed to the extended ignition delay period of B25, increasing the premixed combustion rate and, thus, the high pressure rise rate. Similarly, a higher pressure rise rate for the diesel-biodiesel-ethanol blends has also been observed by Ma et al. (2021), and the reason for that has been ascribed to the extended ignition delay of the fuel blends. The maximum pressure rise rate for all test fuels is below the limit of 1 MPa/°CA (=9 MPa/ms). It is a significant finding regarding smooth engine operation and durability. The pressure rise rate is associated with the engine knock and as its value increases the mechanical and thermal stress on engine components increases (Erdoğan et al., 2019).

The ignition delay period and total combustion duration of the test fuel at maximum load condition are shown in Figure 7. Ignition delay time for DF, B25, B25+NPs50, B25+NPs100, and B25NP150 is 0.89, 1.11, 1.00, 0.89, and 0.89 ms, respectively, while the combustion duration is 9.33, 11.56, 11.33, 10.11, and 10.22 ms with the same order. B25 fuel gives the most extended ignition delay and total combustion duration. B25 fuel with high kinematic viscosity and density, low cetane index, and high boiling point temperature could deteriorate fuel atomization and hence uniformity of air-fuel mixture, which causes a length ignition delay period. Furthermore, because of the lower heat release rate of B25, the total combustion duration is longer than the rest of the fuels. However, by the dispersion of T_iO_2 nanoparticles by 50, 100, and 150 ppm concentrations in B25 fuel, the ignition delay and total combustion periods are slightly shortened. The large surface area of TiO_2 nanoparticles allows a high contact area for fuel and air molecules and enhanced chemical reactivity, shortening the ignition delay time (Mei et al., 2019). Besides, the high ability to conduct the heat of TiO_2 nanoparticles boosts the heat transfer through fuel molecules, speeding up the evaporation of fuel droplets and thereby improving the mixture formation (Ahmed et al., 2020). These factors could become dominant on the lower cetane index of nanofuels, and consequently, the ignition delay is shortened. The lower combustion duration of nanofuels can also be attributed to the high chemical reactivity of nanoparticles, which increases the fuel-burning rate.
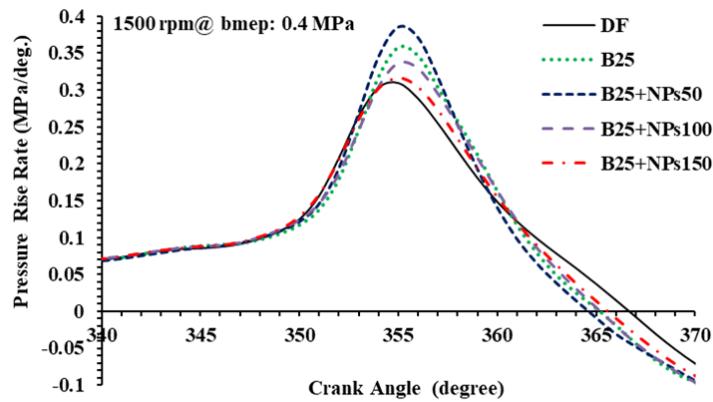
694

Figure 6:
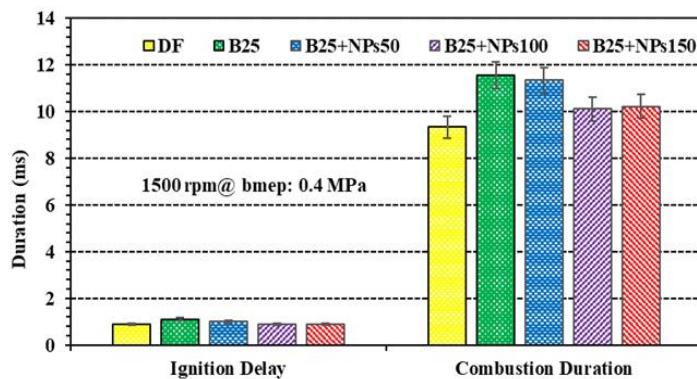*Pressure rise rate curve of test fuels.*

Figure 7:
Ignition delay and total combustion duration of fuels.

3.2. Analysis of Performance Characteristics

Figure 8 shows the brake-specific fuel consumption (bsfc) graph. Due to lower thermal efficiency, brake-specific fuel consumption is high at a low engine load. When the engine load rises for a fixed rotational speed, the increase in effective power exceeds the increase in fuel consumption due to high fuel conversion efficiency; therefore, bsfc diminishes. Therefore, the lowest bsfc is achieved at the engine load of 0.4 MPa for DF, B25, B25+NPs50, B25+NPs100, and B25NP150 following the order 0.2070, 0.2247, 0.2158, 0.2157, 0.2161 kg/kWh. At all load points, B25 fuel gives the highest bsfc among the fuels, and it causes an average increase in the bsfc by 6.78% compared to DF. The reason for this is the worsened fuel-air mixture due to the high viscosity and density of B25 fuel. Therefore, poor combustion occurs, and bsfc increases. Further, high bsfc for B25 is due to the low calorific value of biofuels. However, it is found that bsfc diminishes by adding TiO_2 nanoparticles to B25 fuel. TiO_2 nanoparticles with high calorific value can increase the energy density of the fuel (Örs et al*., 2018), which reduces the amount of injected fuel into the cylinder to produce the same brake power output concerning B25 fuel. The average decrease in bsfc is 0.79, 1.38, and 3.21% with B25+NPs50, B25+NPs100, and B25NP150, respectively, compared to B25 fuel. Besides, the reduction percentage in average bsfc is raised with the increase in TiO_2 dosage in B25 fuel. It may be attributed to improved air-fuel mixing due to the boosted thermal conductivity of fuel and the large contact surface area

between fuel and air. Also, nanofuels could have better spray penetration, which enhances the homogeneity of the mixture and ultimately improves fuel economy (Soukht Saraee et al*.,* 2015). Moreover, the high catalytic activity of TiO_2 nanoparticles speeds up the chemical reactions, and thus, more complete combustion is achieved for nanofuels (Vigneswaran et al*.,* 2021). Consequently, the combination of these factors results in a decrease in bsfc. This finding aligns with similar studies showing that fuel economy is improved with TiO_2-dispersed fuels (Ge et al., 2022; Örs et al., 2018).
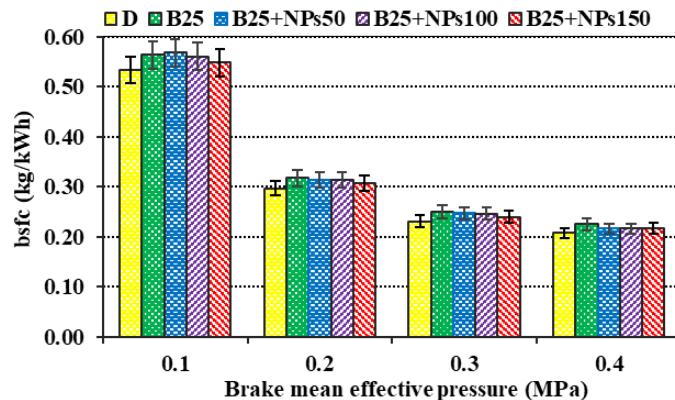

Figure 8:
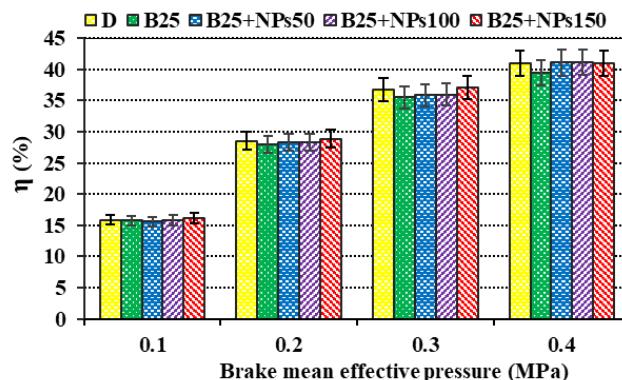*Brake-specific fuel consumption graph*

Figure 9:
Brake-effective efficiency graph

Figure 9 displays the brake-effective efficiency graph for test fuels. When the load increases, brake effective efficiency increases because of high power output and lower heat loss rate (Heywood, 1988). Therefore, the peak brake effective efficiency occurs at the 0.4 MPa load for all test fuels. B25 fuel gives the lowest brake effective efficiency at the entire engine load range, while B25+NPs150 shows the highest among the test fuels. Moreover, the other TiO_2-added fuels are also superior to B25 in fuel conversion efficiency. B25 fuel causes an average decrease in brake effective efficiency by 2.78% compared to DF. The addition of TiO_2 nanoparticles to B25 fuel improves the brake effective efficiency. In addition, it is found that as nanoparticle concentration in the fuel increases, the brake effective efficiency increases even more. For instance, the average increase in brake effective efficiency is 1.83%, 2.11%, and 3.67% for B25+NPs50, B25+NPs100, and B25+NP150, respectively, compared to B25 without nanoparticles. The reasons for the high effective efficiency of nanofuels could be the high chemical reactivity and the excellent ability to conduct the heat of TiO_2 nanoparticles, which is

also highlighted by some researchers (Hameed and Muralidharan, 2023; Kumbhar et al., 2023; Sateesh et al., 2023). The superior thermal conductivity of nanoparticles offers a high heat transfer rate that evaporates the fuel droplets quickly and yields a more homogeneous mixture, resulting in better combustion and, hence, high brake-effective efficiency (Ahmed et al., 2020). Further, nanoparticles can improve fuel oxidation due to their catalytic activity, leading to high fuel conversion efficiency (Sivakumar et al., 2018).

3.3. Exhaust emissions

Figure 10 shows that CO emissions decrease as the bmep increases for all fuels. It is due to elevated combustion temperatures beneficial for CO oxidation to CO_2 (Heywood, 1988). B25 fuel gives the maximum CO emissions at the entire bmep range. It is probably due to its poor injection characteristics and low evaporation behavior, which outweigh the oxygen availability in the fuel structure and reduce the fuel burning rate. Compared to DF, the average percentage increase in CO emissions is 6.77% with B25 fuel. However, CO emission diminishes with the dispersion of TiO_2 nanoparticles into B25 fuel concerning neat B25 fuel, and the minimum CO emission is seen in B25+NP100 test fuel. The large surface area of nanoparticles and the chemical activity of TiO_2 nanoparticles can be the reasons for the reduction in CO emissions. But interestingly, B25+NPs150 fuel produces higher CO emissions than the other nanofuels. It could be attributed to a slight increase in fuel viscosity due to the highest TiO_2 concentration. Nevertheless, B25+NPs150 fuel emits fewer CO emissions than B25 fuel. The average CO emission reduction for 50, 100, and 150 ppm TiO_2 doped fuel is 16.00%, 25.17%, and 5.27%, respectively, compared to B25 fuel. In addition, B25+NPs50 and B25+NPs100 test fuels offer an average reduction in CO emission by 10.32% and 20.11%, respectively, compared to DF.
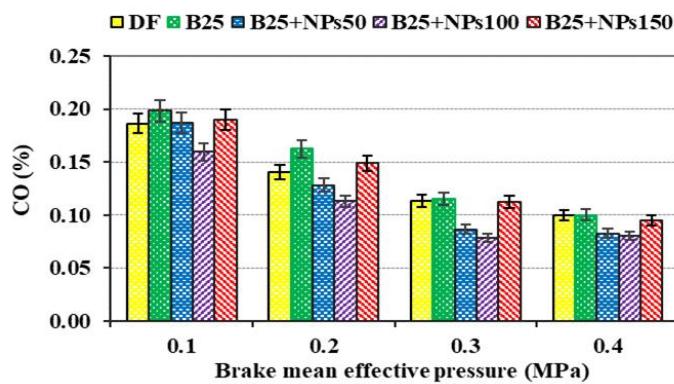

Figure 10:
CO emission for test fuels.

NO_X emissions are generated in several mechanisms in internal combustion engines. However, the thermal NO_X formation pathway is the primary source of NO_X in engines. The measured NO emission of the test fuels according to engine load is illustrated in Figure 11. This figure shows that NO is correlated with engine load. With an increment in engine load, the combustion temperature increases, forming more NO emissions irrespective of which test fuel is used. DF creates the highest NO emission at each engine load condition, whereas B25 produces the lowest. The formation of the highest NO concentration with DF can be due to its high heating value and good fuel injection characteristics. Furthermore, the highest NO emissions for DF can be expressed by its lowest smoke opacity, as presented in Figure 12. Low smoke opacity indicates more complete combustion, hence high cylinder gas temperature (Pulkrabek, 2004). Moreover, a decrease in combustion temperature due to radiation is linked to high soot

concentration (Heywood, 1988). The low radiative heat transfer due to the low soot particle generation for DF promotes a further rise in the flame temperature, which is dominant for NOx formation (Fujimori et al., 2000). On the other hand, B25 fuel with the lowest heating value and high viscosity may worsen the combustion process and reduce combustion temperature, hence less NO formation. Nevertheless, the poor combustion process of B25 fuel is also confirmed by its combustion characteristics, high CO emission, and high smoke opacity. Besides, the high vaporization enthalpy of ethanol in the biofuel mixture has a charge-cooling effect, decreasing temperature throughout the engine cycle. The findings indicate that the combustion temperature dominates NO formation compared to oxygen availability and combustion duration for B25 used in this study. Consequently, B25 fuel diminishes the NO emission on average by 25.33% compared to DF. Regarding the impact of TiO_2 nanoparticles on NO emission, it is found that NO formation is supported mainly due to nanoparticles' high catalytic effect. An increment in TiO_2 concentration in B25 fuel further increases the NO emission. It is because nanoparticles allow more efficient combustion (Jin and Wei, 2023). The percentage increase in mean NO emission is 17.80%, 22.00%, and 23.01% for 50, 100, and 150 ppm TiO_2 concentration relative to B25 fuel. On the other hand, nanofuels still have lower NO emissions than DF. B25+NPs50, B25+NPs100, and B25+NPs150 emit lower NO emissions by 12.03%, 8.89%, and 8.15%, on average, compared to DF.
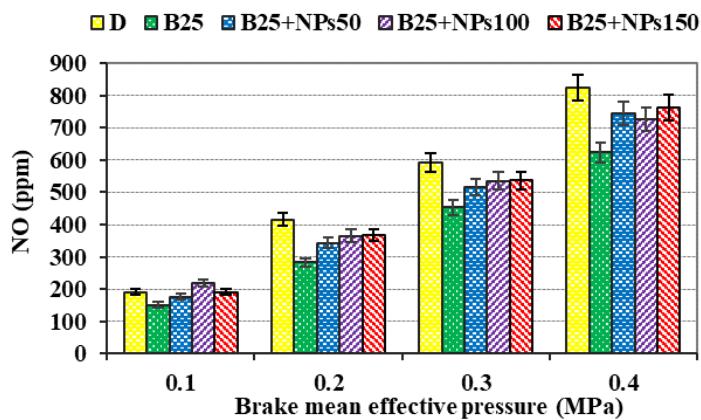

Figure 11:
NO emission for test fuels.

The fuel combustion inside the engine cylinder produces soot particles seen as black smoke in the exhaust. The detected smoke opacity for test fuels is given in Figure 12. Smoke opacity of the exhaust gases increases with engine load due to enlarging the fuel-rich zones as the injected amount of fuel increases (Pulkrabek, 2004). DF's lowest smoke opacity is detected at all engine loads due to its proper mixing with air. B25 fuel and TiO_2 dispersed nanofuels present higher smoke opacity than DF. It is probably due to the formation of a non-uniform mixture because of the biofuel mixture's high viscosity and high boiling point components. Further, the increasing fuel consumption for fuel blends is another factor that affects the smoke opacity. Unsaturated compounds in biofuel mixture and its high water content may cause more soot particles. As a result of the combination of these factors, B25 fuel causes higher smoke opacity by 39.03% on average compared to DF. Nevertheless, smoke opacity is mitigated with the dispersion of TiO_2 nanoparticles in B25 fuel. No consistent trend is observed between smoke opacity and TiO_2 concentration at low and mid-engine load conditions. While at high and full engine loads, the reduction in smoke opacity rises with an increment in nanoparticle concentration. This is because the nanoparticles offer much more catalytic activity at higher engine loads as the cylinder gas temperature is elevated at higher loads (Ashok *et al.,* 2017). It is determined that

the smoke opacity decreases with B25+NPs50, B25+NPs100, and B25+NPs150 by 3.64%, 3.24%, and 16.78%, respectively, on average, compared to B25 without nanoparticles. It can result from the high chemical activity and a large surface area of nanoparticles that promotes more efficient and cleaner combustion (Kumar et al., 2019; Zhang et al., 2023). Additionally, over 90% of soot particles generated within the engine cylinder are oxidized when the gas temperature and oxygen concentration are sufficient (Pulkrabek, 2004). In this regard, nanoparticles can reduce the ignition temperature and increase the oxidation rate of soot particles (Hameed and Muralidharan, 2023). Therefore, fewer soot particles are emitted, and consequently, the opacity of the exhaust gases decreases. Similarly, a considerable reduction in smoke opacity with increased TiO_2 dosage was reported in previous studies. (Kurre et al., 2023; Praveen et al., 2022; Sundar et al., 2022).
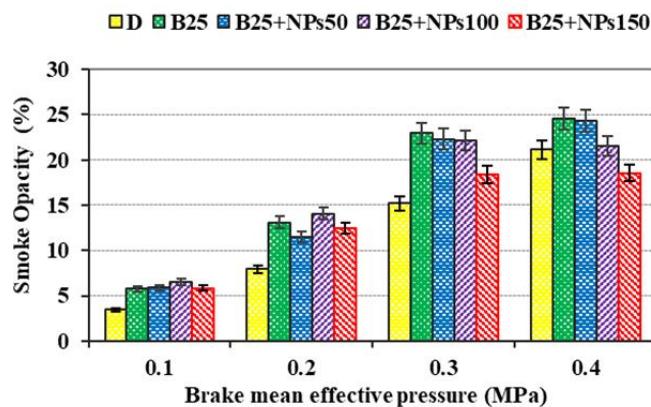

Figure 12:
Smoke opacity for test fuels.

CO_2 emission from test fuels is shown in Figure 13. The lowest CO_2 emission from the test engine is observed with B25 fuel. It leads to less CO_2 emission by 5.73%, on average, compared to DF. Despite its high fuel consumption, B25 fuel diminishes CO_2 emissions because of its low carbon content and inefficient combustion compared to diesel fuel. The addition of TiO_2 nanoparticles increases CO_2 emissions. The B25+NPs50, B25+NPs100, and B25+NPs 150 fuel produce higher CO_2 emission by 5.73%, 6.97%, and 7.06%, respectively on average compared to B25 fuel. The existence of nanoparticles in fuel improves combustion, and thus, high CO_2 emission occurs. Besides, due to the chemical activity of TiO_2 nanoparticles, more CO is converted to CO_2.

The average changes in performance parameters and exhaust emissions for TiO_2 nanoparticles included fuels compared to B25 base fuel are summarised in Table 5. It is seen that all nanofuels offer better engine performance and lower exhaust emissions, except for CO_2 and NO, compared to B25 fuel. However, the average NO emission for B25+NPs50, B25+NPs100, and B25+NPs 150 is lower by 12.03%, 8.89%, and 8.15% than diesel fuel. Additionally, the mean change in CO_2 emission for nanofuels is -0.33%, +0.84%, and +0.92% in the same order, compared to diesel fuel.
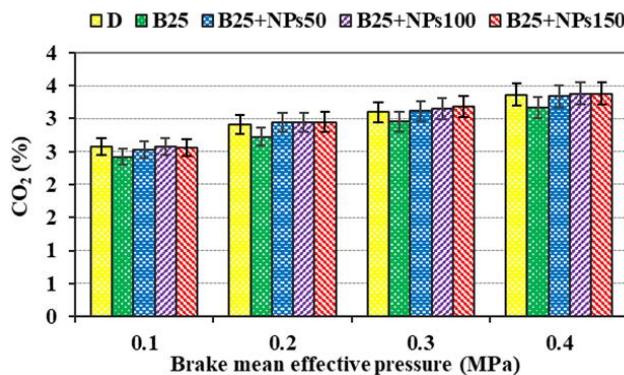
Figure 13:
CO_2 emission for test fuels.

Table 5. The average change in performance and emissions of nanofuels, compared to B25

Parameters	B25+NPs50	B25+NPs100	B25+NPs150
Brake-specific fuel consumption	0.79% ↓	1.38% ↓	3.21% ↓
Brake-effective efficiency	1.83% ↑	2.11% ↑	3.67% ↑
CO	16.00% ↓	25.17% ↓	5.27% ↓
NO	17.80% ↑	22.00% ↑	23.01% ↑
Smoke opacity	3.64% ↓	3.24% ↓	16.78%↓
CO_2	5.73% ↑	6.97% ↑	7.06% ↑

4. CONCLUSIONS

This study is performed to exploit TiO_2 nanoparticles added to a biofuel mixture-diesel blend (B25) to improve its engine combustion, performance, and emissions characteristics. TiO_2 nanoparticles are dispersed in B25 fuel at a dosage rate of 50, 100, and 150 ppm, while diesel fuel (DF) and B25 fuel without nanoparticles are used as reference fuels to compare the findings. It is concluded that:

- Adding TiO_2 nanoparticles to the biofuel mixture-diesel blend raises the maximum cylinder pressure and heat release rate. Besides, the ignition delay and combustion duration decrease with nanoparticle use.
- B25 fuel presents higher bsfc by 5.51%-8.55% than DF. However, TiO_2 nanoparticles result in a considerable decrement in bsfc. The highest average decrease rate in bsfc is observed with 150 ppm TiO_2 concentration by 3.21% compared to B25. Similarly, it increases brake effective efficiency by 3.67%, compared to B25.
- Regarding the exhaust emissions, the highest CO emission is measured with B25 fuel, which is higher by 6.77% than DF, on average. On the other hand, CO emission is reduced by adding TiO_2 nanoparticles to B25 fuel.
- Including TiO_2 nanoparticles in B25 fuel decreases the smoke opacity. The smoke opacity is reduced up to 24.56% with B25+NPs150 fuel compared to B25 fuel.

- NO emission increases with TiO_2 usage. Also, as the TiO_2 concentration increases, the NO emission further increases. The maximum average increase of 23.01% in NO emission for B25+NPs150 fuel is found. Nonetheless, TiO_2-dispersed fuels present lower NO emission than DF.
- 150 ppm TiO_2 concentration is superior regarding performance characteristics and the lowest smoke opacity to others. Its average NO emission is comparable to that of B25+NPs100 with a slightly higher value. But B25+NPs150 provides a higher reduction in smoke opacity. It is advantageous regarding the NO_X-soot trade-off; thus, B25+NPs 150 is preferable.
- Considering all the results, it can be concluded that B25+NPs150 fuel might be appropriate for stationary diesel engines. However, the high cost of TiO_2 nanoparticles and their toxic effects must also be considered.

Overall, it is concluded that using TiO_2 nanoparticles as a fuel additive is a feasible way to overcome the performance issues of biofuels. The readjustment of engine settings may allow the further benefit of nanoparticle-doped biofuels. Research in this direction can be conducted.

ACKNOWLEDGEMENTS

CONFLICT OF INTERESTS

The author declares that he has no actual, potential, or perceived conflict of interest for this article.

AUTHOR CONTRIBUTION

The author confirms sole responsibility for preparing the manuscript, including designing and performing experiments, data collection, analysis, interpretation of results, and writing and editing the manuscript.

REFERENCES

1. Agarwal, A. K. (2007) Biofuels (alcohols and biodiesel) applications as fuels for internal combustion engines, *Progress in Energy and Combustion Science*, *33*(3), 233–271. https://doi.org/https://doi.org/10.1016/j.pecs.2006.08.003

2. Ahmed, A., Shah, A. N., Azam, A., Uddin, G. M., Ali, M. S., Hassan, S., Ahmed, H., and Aslam, T. (2020) Environment-friendly novel fuel additives: Investigation of the effects of graphite nanoparticles on performance and regulated gaseous emissions of CI engine, *Energy Conversion and Management*, 211, 112748. https://doi.org/10.1016/j.enconman.2020.112748

3. Ashok, B., Nanthagopal, K., Subbarao, R., Johny, A., Mohan, A., and Tamilarasu, A. (2017) Experimental studies on the effect of metal oxide and antioxidant additives with Calophyllum Inophyllum Methyl ester in compression ignition engine, *Journal of Cleaner Production*, 166, 474–484. https://doi.org/https://doi.org/10.1016/j.jclepro.2017.08.050

4. Çakmak, A., Yeşilyurt, M. K., Erol, D., and Doğan, B. (2022) The experimental investigation on the impact of n-octanol in the compression-ignition engine operating with

biodiesel/diesel fuel blends: exergy, exergoeconomic, environmental analyses, *Journal of Thermal Analysis and Calorimetry*. https://doi.org/10.1007/s10973-022-11357-w

5. Çakmak, A. (2022) Experimental Investigation On Exploiting The Biofuels Blend And *Improving* Its Usability By Adding TiO₂ Nanoparticles. *The Proceedings of 16th International Combustion Symposium (INCOS2022), September 08-11, 2022, Aydın, Türkiye*, 355–362. https://doi.org/ISBN 978-625-00-9337-5

6. Çakmak, A. ve Özcan, H. (2022) Bor oksit nanoparçacıklarının dizel yakıt katkısı olarak kullanılabilirliğinin araştırılması, Journal of Boron, 7(1), 433-442. https://doi.org/10.30728/boron.1021667

7. Erdoğan, S., Balki, M. K., and Sayin, C. (2019) The effect on the knock intensity of high viscosity biodiesel use in a DI diesel engine, *Fuel*, 253, 1162–1167. https://doi.org/10.1016/j.fuel.2019.05.114

8. European Commission. (2014). *Communication from the Commission to the European* Parliament*, the Council,* the *European Economic and Social Committee and the Committee of the Regions. A policy framework for climate and energy in the period from 2020 to 2030*. Accessed March 2023. https://eur-lex.europa.eu/legal-content/EN/ALL/?uri=CELEX:52014DC0015

9. Fujimori, T., Hamano, Y., and Sato, J. (2000) Radiative heat loss and NOx emission of turbulent jet flames in preheated air up to 1230 K, *Proceedings of the Combustion Institute*, 28(1), 455–461. https://doi.org/https://doi.org/10.1016/S0082-0784(00)80243-X

10. Ge, S., Brindhadevi, K., Xia, C., Salah Khalifa, A., Elfasakhany, A., Unpaprom, Y., and Whangchai, K. (2022) Performance, combustion and emission characteristics of the CI engine fueled with Botryococcus braunii microalgae with addition of TiO2 nanoparticle, *Fuel*, 317, 121898. https://doi.org/https://doi.org/10.1016/j.fuel.2021.121898

11. Gülüm, M. (2023) Performance, combustion and emission characteristics of a diesel engine fuelled with diesel fuel + corn oil + alcohol ternary blends, *Environmental Science and Pollution Research*. https://doi.org/10.1007/s11356-023-26053-x

12. Hadhoum, L., Zohra Aklouche, F., Loubar, K., and Tazerout, M. (2021) Experimental investigation of performance, emission and combustion characteristics of olive mill wastewater biofuel blends fuelled CI engine, *Fuel*, 291, 120199. https://doi.org/https://doi.org/10.1016/j.fuel.2021.120199

13. Hameed, A. Z., and Muralidharan, K. (2023) Performance, Emission, and Catalytic Activity Analysis of AI₂O₃ and CeO₂ Nano-Additives on Diesel Engines Using Mahua Biofuel for a Sustainable Environment, *ACS Omega*, 8(6), 5692–5701. https://doi.org/10.1021/acsomega.2c07193

14. Heywood, J. B. (1988) *Internal combustion engine fundamentals.* McGraw-Hill.

15. Hoang, A. T. (2021) Combustion behavior, performance and emission characteristics of diesel engine fuelled with biodiesel containing cerium oxide nanoparticles: A review, *Fuel Processing Technology*, 218, 106840. https://doi.org/https://doi.org/10.1016/j.fuproc.2021.106840

16. Jin, C., and Wei, J. (2023) The combined effect of water and nanoparticles on diesel engine *powered* by biodiesel and its blends with diesel: A review, *Fuel*, 343, 127940. https://doi.org/https://doi.org/10.1016/j.fuel.2023.127940

17. Khan, M. M., Sharma, R. P., Kadian, A. K., and Hasnain, S. M. M. (2022) An assessment of alcohol inclusion in various *combinations* of biodiesel-diesel on the performance and

exhaust emission of modern-day compression ignition engines – A review, *Materials Science for Energy Technologies*, 5, 81–98. https://doi.org/https://doi.org/10.1016/j.mset.2021.12.004

18. Kumar, M. (2020) Social, economic, and environmental impacts of renewable energy resources, In *Wind solar hybrid* renewable *energy system* (Vol. 1). IntechOpen London, UK. https://doi.org/10.5772/intechopen.89494

19. Kumar, S., Dinesha, P., and Bran, I. (2019) Experimental investigation of the effects of nanoparticles as an additive in diesel and biodiesel fuelled engines: a review, *Biofuels*, *10*(5), 615–622. https://doi.org/10.1080/17597269.2017.1332294

20. Kumbhar, V., Pandey, A., Sonawane, C. R., Panchal, H., and Ağbulut, Ü. (2023) Numerical and experimental investigation of the influence of various metal-oxide-based nanoparticles on performance, combustion, and emissions of CI engine fuelled with tamarind seed oil methyl ester, *Energy*, 265, 126258. https://doi.org/https://doi.org/10.1016/j.energy.2022.126258

21. Kurre, S. K., Yadav, J., Khan, M. K., Yadav, P., Munaf Dhebar, M., and Rawat, B. S. (2023) Experimental evaluation of performance and emission of diesel engine fueled with nano-material titanium dioxide (TiO_2) nanoparticles supplemented diesel-biodiesel-ethanol blends. *Materials Today: Proceedings*. https://doi.org/https://doi.org/10.1016/j.matpr.2023.01.306

22. Ma, Q., Zhang, Q., Liang, J., Yang, C., and Materials, A. (2021) The performance and emissions characteristics of diesel/biodiesel/alcohol blends in a diesel engine, *Energy Reports*, 7, 1016–1024. https://doi.org/https://doi.org/10.1016/j.egyr.2021.02.027

23. Mei, D., Zuo, L., Adu-Mensah, D., Li, X., and Yuan, Y. (2019) Combustion characteristics and emissions of a common rail diesel engine using nanoparticle-diesel blends with carbon nanotube and molybdenum trioxide, *Applied Thermal Engineering*, 162, 114238. https://doi.org/10.1016/j.applthermaleng.2019.114238

24. Santhosh, N., Afzal, A., Ağbulut, Ü., Alahmadi, A. A., Gowda, A. C., Alwetaishi, M., ... and Hoang, A. T. . (2023) Poultry fat biodiesel as a fuel substitute in diesel-ethanol blends for DI-CI engine: Experimental, modeling and optimization, *Energy*, 126826. https://doi.org/https://doi.org/10.1016/j.energy.2023.126826

25. Niculescu, R., Clenci, A., and Iorga-Siman, V. (2019) Review on the Use of Diesel–Biodiesel–Alcohol Blends in Compression Ignition Engines, In *Energies* (Vol. 12, Issue 7). https://doi.org/10.3390/en12071194

26. Örs, I., Sarıkoç, S., Atabani, A. E. E., Ünalan, S., and Akansu, S. O. O. (2018) The effects on performance, combustion and emission characteristics of DICI engine fuelled with TiO2 nanoparticles addition in diesel/biodiesel/n-butanol blends, *Fuel*, 234, 177–188. https://doi.org/10.1016/J.FUEL.2018.07.024

27. Praveen, A., Krupakaran, R. L., Lakshmi Narayana Rao, G., and Balakrishna, B. (2022) An assessment of the TiO2 nanoparticle concentration in the C. inophyllum biodiesel blend on the engine characteristics of a DI diesel engine, *International Journal of Ambient Energy*, 43(1), 5464–5477. https://doi.org/10.1080/01430750.2021.1953584

28. Pulkrabek, W. W. (2004) *Engineering Fundamentals of the Internal Combustion Engine* (Second). Published by Pearson.

29. Sateesh, K. A., Yaliwal, V. S., Banapurmath, N. R., Soudagar, M. E. M., Yunus Khan, T. M., Harari, P. A., El-Shafay, A. S., *Mujtaba*, M. A., Elfaskhany, A., and Kalam, M. A. (2023) Effect of MWCNTs nano-additive on a dual-fuel engine characteristics utilizing

dairy scum oil methyl ester and producer gas, *Case Studies in Thermal Engineering*, *42*, 102661. https://doi.org/https://doi.org/10.1016/j.csite.2022.102661

30. Sivakumar, M., Shanmuga Sundaram, N., Ramesh kumar, R., and Syed Thasthagir, M. H. (2018) Effect of aluminium oxide nanoparticles blended pongamia methyl ester on performance, combustion and emission characteristics of diesel engine, *Renewable Energy*, 116, 518–526. https://doi.org/10.1016/J.RENENE.2017.10.002

31. Soukht Saraee, H., Jafarmadar, S., Taghavifar, H., and Ashrafi, S. J. (2015) Reduction of emissions and fuel consumption in a compression ignition engine using nanoparticles, *International Journal of Environmental Science and Technology*, 12(7), 2245–2252. https://doi.org/10.1007/s13762-015-0759-4

32. Suhaimi, H., Adam, A., Mrwan, A. G., Abdullah, Z., Othman, M. F., Kamaruzzaman, M. K., and Hagos, F. Y. (2018) Analysis of combustion characteristics, engine performances and emissions of long-chain alcohol-diesel fuel blends, *Fuel*, 220, 682–691. https://doi.org/https://doi.org/10.1016/j.fuel.2018.02.019

33. Sundar, S. P., Palanimuthu, V., Sathyamurthy, R., Hemalatha, D., Kumar, R. S., Bharathwaaj, R., Vasanthaseelan, S., and Chamkha, A. (2022) Feasibility study of neat plastic oil with TiO2 nanoadditive as an alternative fuel in internal combustion engine, *Journal of Thermal Analysis and Calorimetry*, 147(3), 2567–2578. https://doi.org/10.1007/s10973-021-10657-x

34. Uslu, S., Simsek, S., and Simsek, H. (2023) RSM modeling of different amounts of nano-TiO_2 supplementation to a diesel engine running with hemp seed oil biodiesel/diesel fuel blends. *Energy*, *266*, 126439. https://doi.org/https://doi.org/10.1016/j.energy.2022.126439

35. Venu, H., Raju, V. D., Lingesan, S., and Elahi M Soudagar, M. (2021) Influence of Al_2O_3nano additives in ternary fuel (diesel-biodiesel-ethanol) blends operated in a single cylinder diesel engine: Performance, combustion and emission characteristics, *Energy*, 215, 119091. https://doi.org/10.1016/j.energy.2020.119091

36. Vigneswaran, R., Balasubramanian, D., and Sastha, B. D. S. (2021) Performance, emission and combustion characteristics of unmodified diesel engine with titanium dioxide (TiO_2) nano particle along with water-in-diesel emulsion fuel, *Fuel*, 285, 119115. https://doi.org/https://doi.org/10.1016/j.fuel.2020.119115

37. Yilbasi, Z., Yesilyurt, M. K., Arslan, M., and Yaman, H. (2023) Understanding the performance, emissions, and combustion behaviors of a DI diesel engine using alcohol/hemp seed oil biodiesel/diesel fuel ternary blends: Influence of long-chain alcohol type and concentration, *Science and Technology for Energy Transition*, 78, 5. https://doi.org/10.2516/stet/2023003

38. Yusuf, A. A., Dankwa Ampah, J., Soudagar, M. E. M., Veza, I., Kingsley, U., Afrane, S., Jin, C., Liu, H., Elfasakhany, A., and Buyondo, K. A. (2022) Effects of hybrid nanoparticle additives in n-butanol/waste plastic oil/diesel blends on combustion, particulate and gaseous emissions from diesel engine evaluated with entropy-weighted PROMETHEE II and TOPSIS: Environmental and health risks of plastic waste, *Energy Conversion and Management*, 264, 115758. https://doi.org/https://doi.org/10.1016/j.enconman.2022.115758

39. Zhang, Y., Gao, S., Zhang, Z., Li, W., Yuan, T., Tan, D., Duan, L., and Yang, G. (2023) A comprehensive review on combustion, performance and emission aspects of higher alcohols and its additive effect on the diesel engine, *Fuel*, 335, 127011. https://doi.org/https://doi.org/10.1016/j.fuel.2022.127011